Electronic Supplementary Information

When NiO@Ni Meets WS_2 Nanosheet Array: A Highly Efficient and Ultra-Stable Electrocatalyst for Overall Water Splitting

Dewen Wang,[†,‡] Qun Li,[†,‡] Ce Han[†], Zhicai Xing,*[,†] and Xiurong Yang*[,†]

[†]State Key Laboratory of Electroanalytical Chemistry, Changchun Institute of Applied Chemistry, Chinese Academy of Sciences, Changchun 130022, Jilin, China

[‡]University of Science and Technology of China, Hefei 230026, China

*E-mail: xingzc@ciac.ac.cn; xryang@ciac.ac.cn

Experimental Section

Materials

CC was purchased from Hongshan District, Wuhan Instrument Surgical Instruments Business, China. $Na_2WO_4 \cdot 2H_2O$, HCl, $H_2C_2O_4$, KOH, $(NH_4)_2SO_4$ and $NiSO_4 \cdot 6H_2O$ were purchased from Beijing Chemical Corp. Pt/C (20 wt% Pt on Vulcan XC-72R), Nafion (5 wt%) and RuO_2 were purchased from Sigma–Aldrich. Powdered sulfur was purchased from Alfa Aesar. All chemicals were used as received without further purification. The water used throughout all experiments was purified through a Millipore system.

Synthesis of WO_3/CC

WO_3/CC was synthesized according to previously reported method.[1]

Synthesis of WS_2/CC

The as obtained WO_3/CC was put in a porcelain boat and powdered sulfur (1g) was put in another porcelain boat, then put them in a tube furnace and calcined at 600 ℃ for 2 h with temperature rise speed of 10 °C min^{-1} under Ar atmosphere. After the tube furnace cooled down to room temperature, the WS_2/CC could be taken out, and the loading of WS_2/CC was 18.8 mg cm^{-2}.

Synthesis of NiO@Ni/WS_2/CC

The electrodeposition of Ni on WS_2/CC was carried out in a three-electrode cell (WS_2/CC, working electrode; a graphite plate, counter electrode; Ag/AgCl, reference electrode). The electrodeposition was performed by cyclic voltammetry over the potential window of -0.2 to -1.4 V (cycles: 30; scan rate: 50 mV s^{-1}) in 0.1 M

$Ni_2SO_4 \cdot 6H_2O$ aqueous solution. All these procedures were carried out at 25 °C under nitrogen protection. After electrodeposition, $Ni/WS_2/CC$ was removed, rinsed by deionized water, and dried in the oven at 80 °C for 30 min for obtaining $NiO@Ni/WS_2/CC$, the eventually loading of $NiO@Ni/WS_2$ was 21.6 mg cm^{-2}. The reference sample, NiO@Ni/CC (loading: 2.8 mg cm^{-2}), was prepared through a similar method using CC as the working electrode, $Ni/WS_2/CC$ was prepared without drying and $NiO/WS_2/CC$ was prepared through drying in the oven at 200 °C for 60 min.

Materials characterizations

Powder XRD data were acquired with a RigakuD/MAX 2550 diffractometer with Cu Ka radiation (l=1.5413). SEM measurements were performed with a XL30 ESEM FEG microscope at an accelerating voltage of 20 kV. TEM measurements were made with a Hitachi H-8100 electron microscope (Hitachi, Tokyo, Japan) with an accelerating voltage of 200 kV. XPS measurements were performed with an ESCALABMK II X-ray photoelectron spectrometer by using Mg as the exciting source. Raman data was obtained on lab RAM ARAMIS Raman spectrometer with 785 nm wavelength incident laser light. X-ray absorption fine structure (XAFS) spectroscopy experiment was carried out at 1W2B end station, Beijing Synchrotron Radiation Facility (BSRF). The Ni K-edge and W K-edge spectra were collected at room temperature in transmission mode. The BET surface area was measured on a Quantachrome NOVA 1000 system at liquid N_2 temperature.

Electrochemical measurements

All electrochemical measurements were performed with a CHI660D electrochemical analyzer (CH Instruments, Inc., Shanghai) at room temperature. NiO@Ni/WS_2/CC was directly used as the working electrode, a saturated calomel electrode (SCE) as the reference electrode, and graphite rod as the counter electrode. Potentials were referenced to a reversible hydrogen electrode (RHE) by adding a value of (0.242 + 0.059 pH) V. RuO_2 and Pt/C ink was prepared by dispersing 10 mg of RuO_2 or Pt/C in 500 μL of ethanol with 5 μL of 5 wt % Nafion solution, then the catalyst ink was loaded onto CC surface and air-dried at room temperature. The ohmic potential drop (*iR*) losses that arise from the solution resistance were all corrected. Tafel plots of the overpotential *vs*. log (current density) are recorded with the linear portions at low overpotential fitted to the Tafel equation ($\eta = a + b \log j$, where η is the overpotential, j is the cathodic current density, and b is the Tafel slope). The stability test of the NiO@Ni/WS_2/CC was also performed using a typical three electrodes system. The capacitances of the double layer (C_{dl}) at the solid−liquid interface of materials were measured by CVs collecting between -0.1 V and -0.2 V *vs* RHE in 1.0 M KOH, where the current response should be only due to the charging of the double layer.

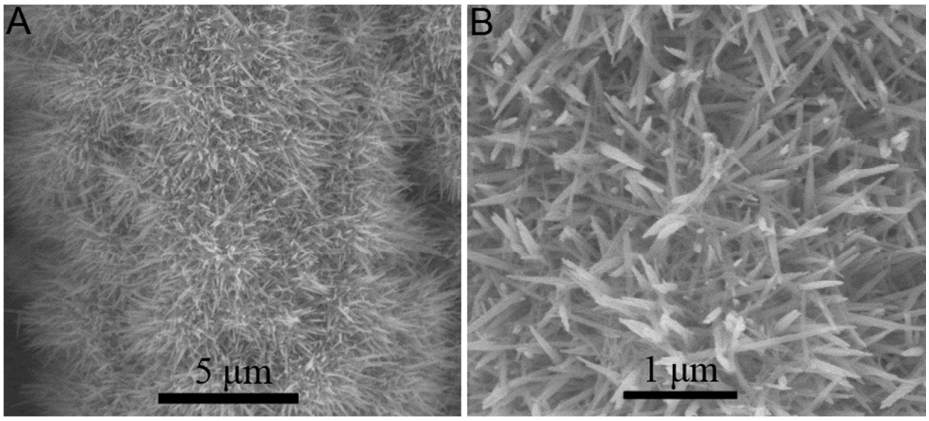

Figure S1. The SEM images of WO_3/CC nanowires at (A) low and (B) high magnification.

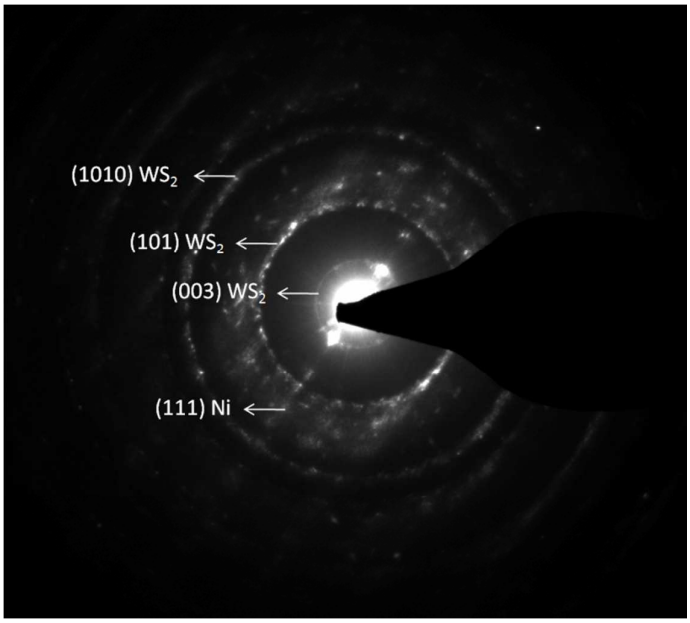

Figure S2. SAED pattern of NiO@Ni/WS_2.

Figure S3. STEM image of a NiO@Ni/WS_2 nanosheet.

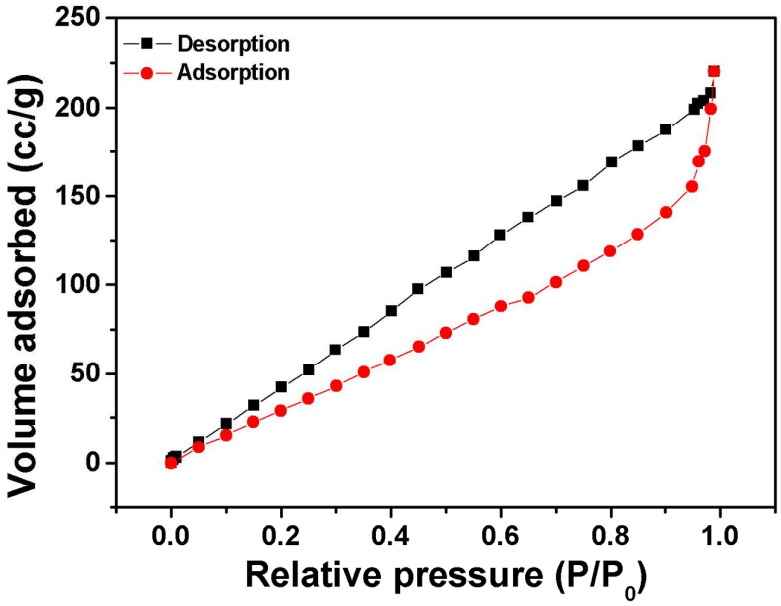

Figure S4. Nitrogen adsorption/desorption isotherm of the NiO@Ni/WS_2/CC electrocatalyst.

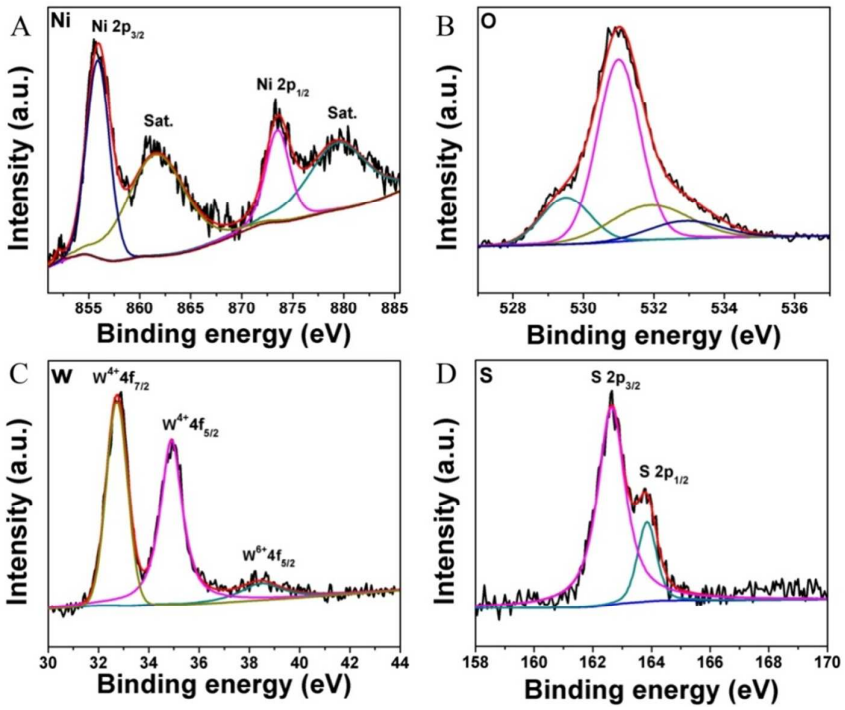

Figure S5. XPS spectra in the (A) Ni 2p, (B) O 1s, (C) W 4f and (D) S 2p regions for NiO@Ni/WS_2/CC.

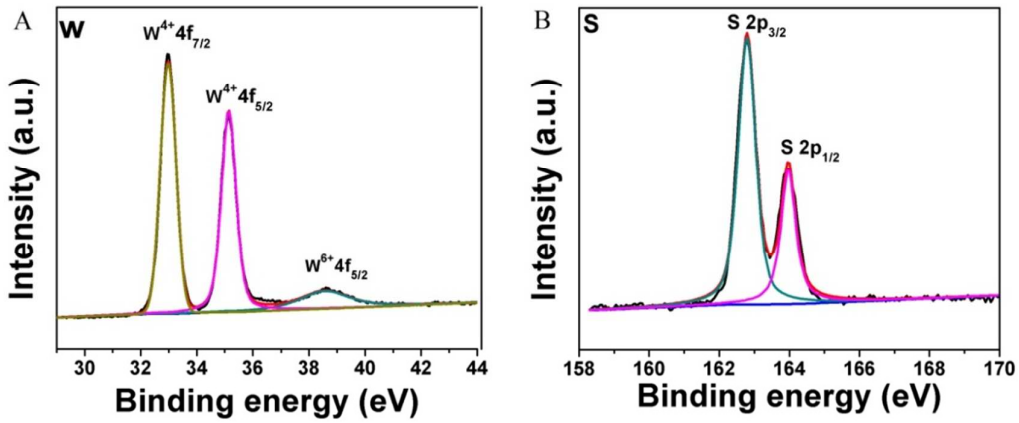

Figure S6. XPS spectra in the (A) W 4f and (B) S 2p regions for WS_2/CC.

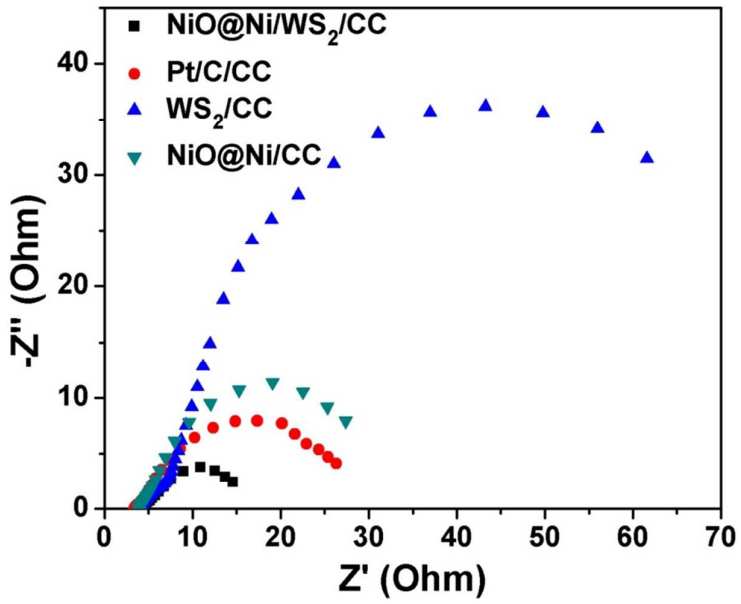

Figure S7. Nyquist plots of electrochemical impedance spectra of NiO@Ni/WS_2/CC, Pt/C/CC, WS_2/CC and NiO@Ni/CC at overpotential of 60 mV.

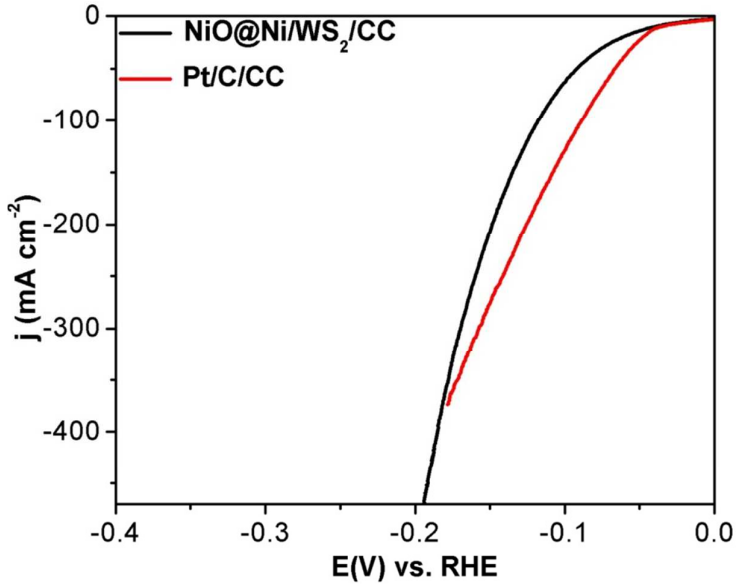

Figure S8. LSV curves for NiO@Ni/WS_2/CC and Pt/C/CC at a scan rate of 5 mV s^{-1} for HER.

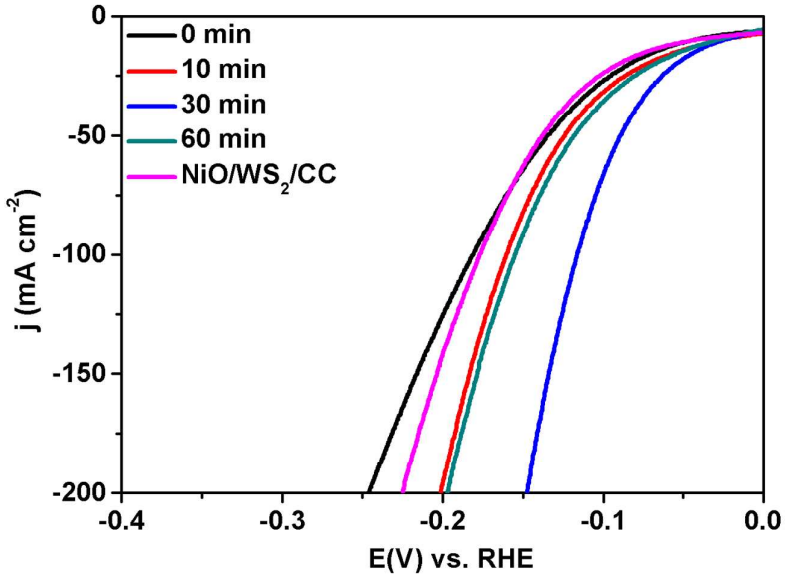

Figure S9. LSV curves for $Ni/WS_2/CC$ at different oxidation times and $NiO/WS_2/CC$ with a scan rate of 5 mVs^{-1} for HER.

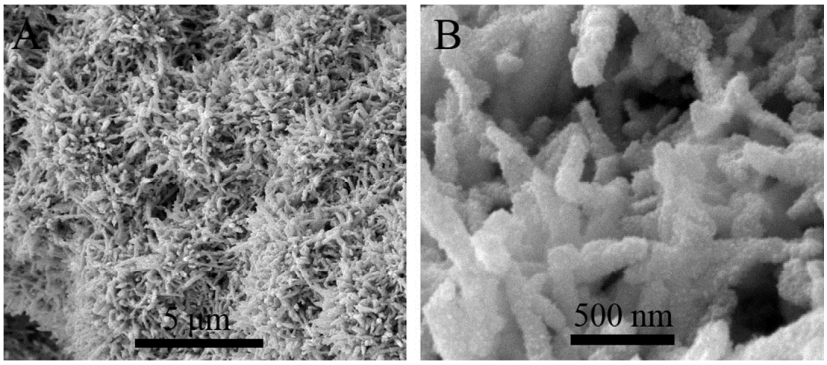

Figure S10. The SEM images of $NiO@Ni/WS_2/CC$ at (A) low and (B) high magnification after HER electrolysis.

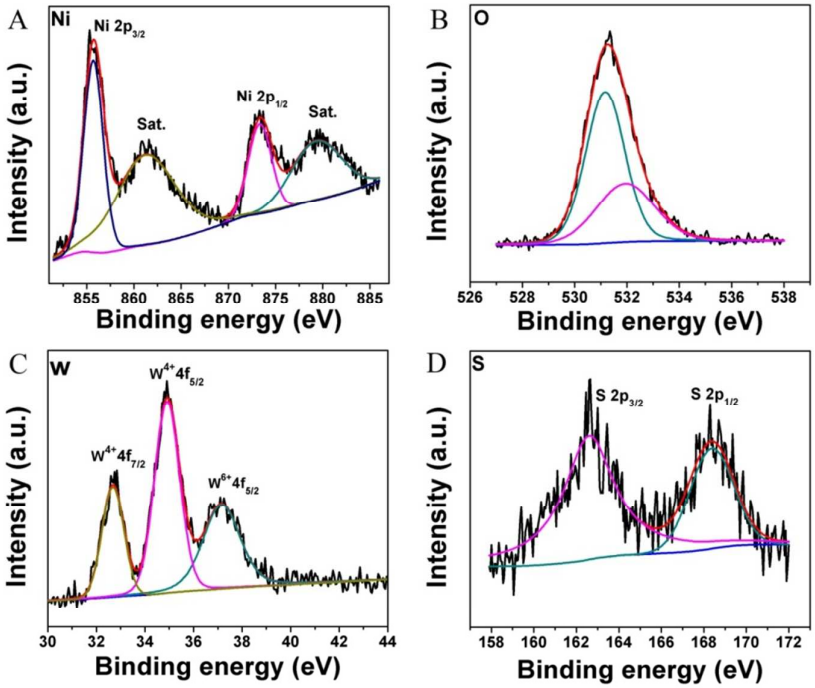

Figure S11. XPS survey spectra of NiO@Ni/WS_2/CC for post-HER test (A) Ni 2p, (B) O 1s, (C) W 4f and (D) S 2p.

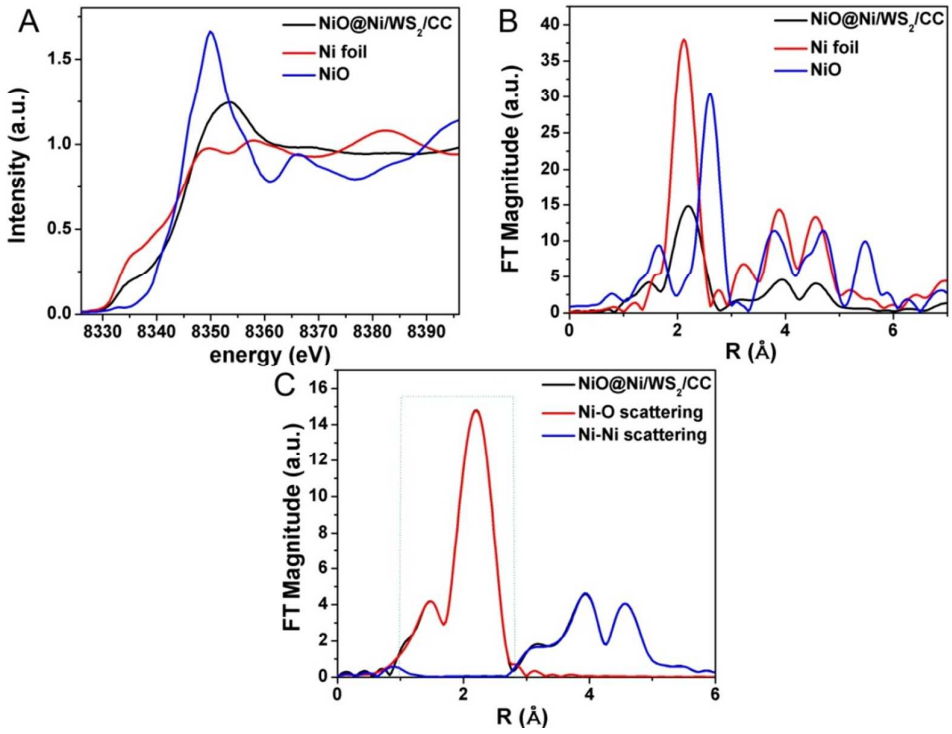

Figure S12. (A) Ni K-edge XANES spectra and (B) Fourier transforms of k3-weighted Ni K-edge EXAFS spectra for NiO@Ni/WS_2/CC after HER test, Ni foil, and NiO. (C) Observed (black line) and calculated (red and blue line) Fourier transforms of k3-weighted Ni K-edge EXAFS spectra for NiO@Ni/WS_2/CC after HER test.

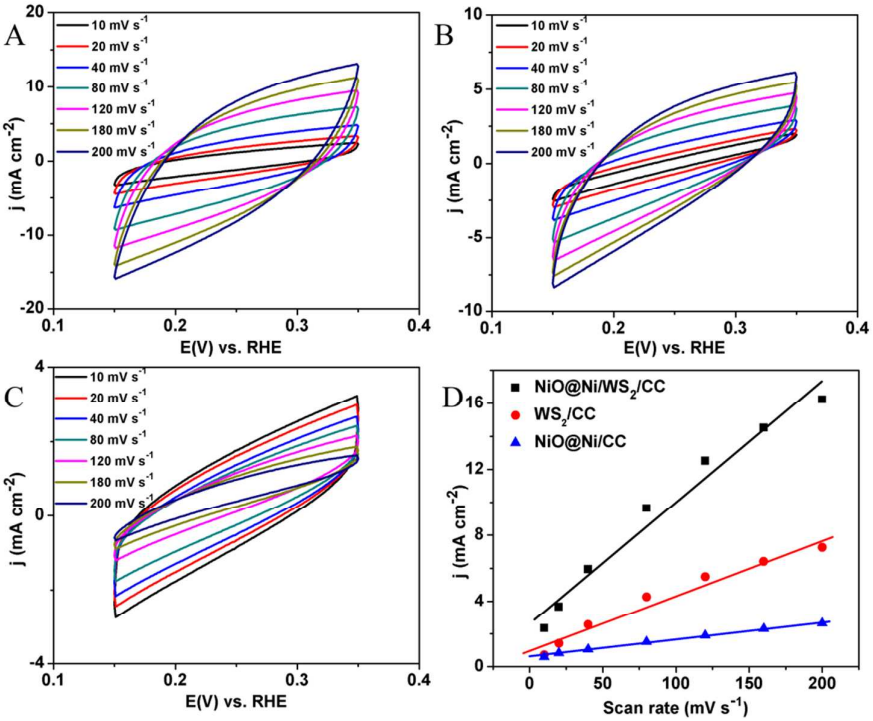

Figure S13. CVs for (A) NiO@Ni/WS_2/CC, (B) WS_2/CC and (C) NiO@Ni/CC. (D) The corresponding capacitive currents at 0.25 V as a function of scan rate for NiO@Ni/WS_2/CC, WS_2/CC and NiO@Ni/CC.

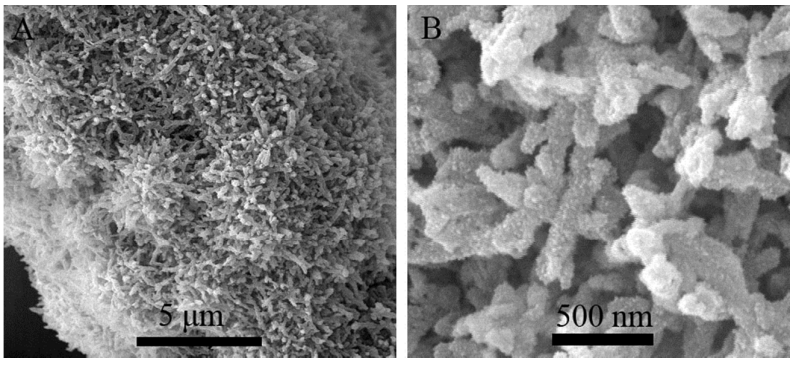

Figure S14. SEM images of NiO@Ni/WS_2/CC at (A) low and (B) high magnification after OER electrolysis.

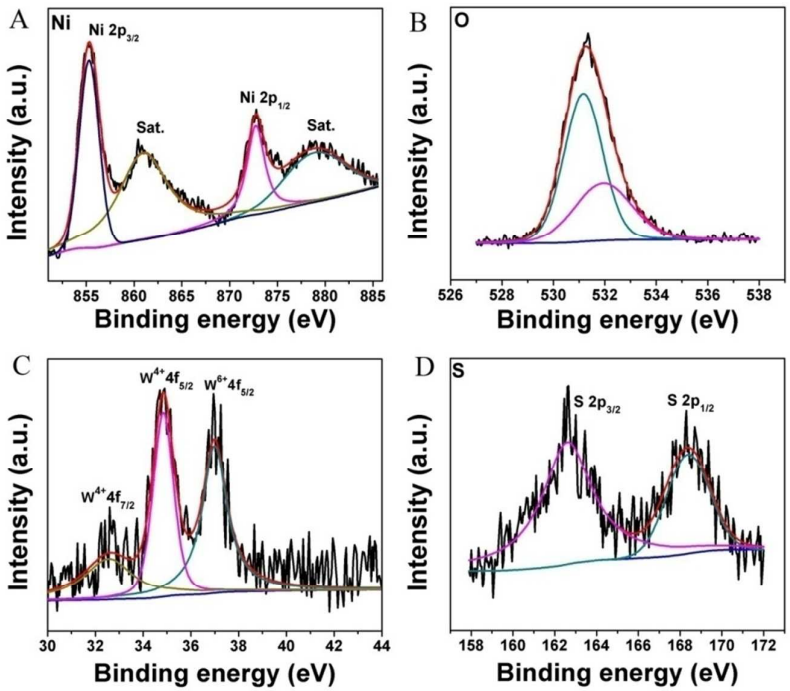

Figure S15. XPS survey spectra of NiO@Ni/WS_2/CC for post-OER test (A) Ni 2p, (B) O 1s, (C) W 4f and (D) S 2p.

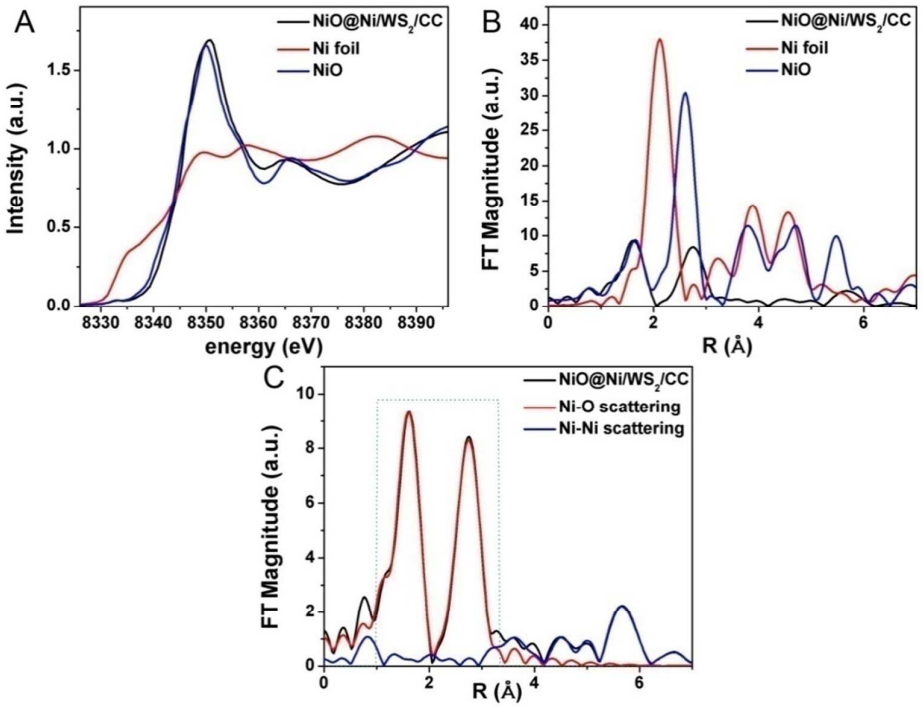

Figure S16. (A) Ni K-edge XANES spectra and (B) Fourier transforms of k3-weighted Ni K-edge EXAFS spectra for NiO@Ni/WS_2/CC after OER test, Ni foil and NiO. (C) Observed (black line) and calculated (red and blue line) Fourier transforms of k3-weighted Ni K-edge EXAFS spectra for NiO@Ni/WS_2/CC after OER test.

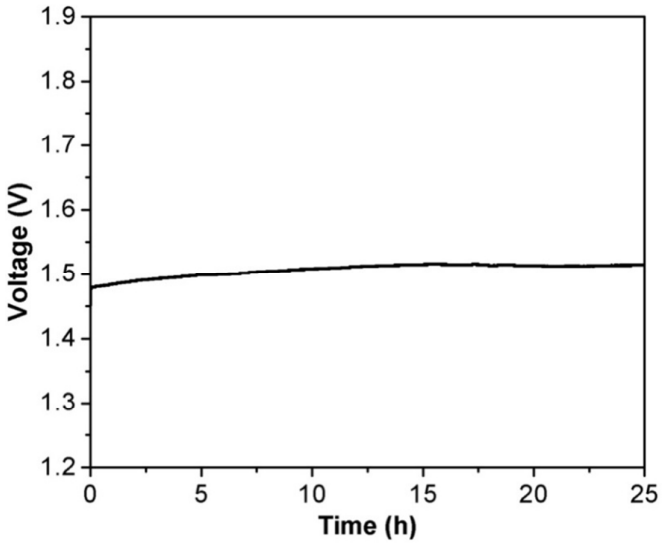

Figure S17. Chronopotentiometric curve of water electrolysis for

NiO@Ni/WS_2/CC||NiO@Ni/WS_2/CC with a constant current density of 10 mA cm^{-2}.

Table S1 EXAFS fitting parameters at the Ni K-edge for various samples.

Sample	Shell	N^a	R(Å)^b	σ^2(Å$^2\cdot10^3$)^c	ΔE^0(eV)^d	R factor (%)
NiO@Ni/WS_2/CC	Ni−O	1.8	2.04	7.5	-4.1	1.07
	Ni−Ni (O-bridged)	7.2	2.48	6.8	-6.6	
NiO@Ni/WS_2/CC post-HER test	Ni−O	2.4	1.87	8.0	-9.0	0.20
	Ni-S	1.3	2.31	2.0	8.8	
	Ni−Ni (O-bridged)	3.5	2.56	5.7	10.0	
NiO@Ni/WS_2/CC post-OER test	Ni−O	6.6	2.05	6.3	-3.7	0.36
	Ni−Ni (O-bridged)	6.5	3.09	9.0	-1.1	
NiO	Ni−O	6.0	2.08	7.4	−2.5	1.55
	Ni−Ni (O-bridged)	12.0	2.95	6.5		
Ni-foil	Ni−Ni (in metallic state Ni)	12	2.48	5.9	−6.1	1.92

N^a: coordination numbers; R(Å)^b: bond distance; σ^2(Å$^2\cdot10^3$)^c: Debye-Waller factors; ΔE^0(eV)^d: the inner potential correction. S_0^2 for Ni-Ni is 0.92, For Ni-O is 0.88, were obtained from the experimental EXAFS fit of Ni-foil/NiO references by fixing CN as the known crystallographic value and were fixed to all the samples.

Table S2 Comparison of selected non-noble metal based HER electrocatalysts in alkaline media.

Catalysts	Electrolyte	j (mA cm^{-2})	η (mV)	Reference
NiO@Ni/WS_2/CC	1 M KOH	10	40	This work
		20	60	
		100	117	
Co-P film	1 M KOH	10	94	*Angew. Chem. Int. Ed.* **2015**, *54,* 6251.
		20	115	
		100	158	
Ni_2P	1 M KOH	20	205	*J. Am. Chem. Soc.* **2013**, *135*, 9267.
Fe-CoP/Ti	1 M KOH	10	78	*Adv. Mater.* **2017**, *29,* 1602441.
		100	164	
NiO/Ni-CNT	1 M KOH	10	~100	*Nat. Commun.* **2014**, *5,* 4695.
CoO_x@CN hybrids	1 M KOH	10	200	*J. Am. Chem. Soc.* **2015**, *137*, 2688.
Amorphous MoS_x	1 M KOH	10	540	*Chem. Sci.* **2011**, *2,* 1262.
Ni-Mo nanopowder	1 M NaOH	10	80	*ACS Catal.* **2013**, ***3,*** 166.
MnNi	1 M KOH	10	360	*Adv. Funct. Mater.* **2015**, *25*, 393.

Table S3 Comparison of selected non-noble metal based OER electrocatalysts in alkaline media.

Catalysts	Electrolyte	j (mA cm^{-2})	η (mV)	Reference
NiO@Ni/WS_2/CC	1.0 M KOH	50	347	this work
$NiFeO_x$ film	1.0 M NaOH	10	>350	*J. Am. Chem. Soc.* **2013**, *135*, 16977.
Fe-Ni oxides	1.0 M KOH	10	>375	*ACS Catal.* **2012**, *2*, 1793.
Ni–Co-mixed oxide nanocages	1.0 M KOH	10	~380	*Adv. Mater.* **2016**, *28*, 4601.
NiCo LDH	1.0 M KOH	10	367	*Nano Lett.* **2015**, *15*, 1421.
MnO_x/Au	0.1 M KOH	10	>480	*J. Am. Chem. Soc.* **2014**, *136,* 4920.
Ni_3S_2/Ni	1.0 M KOH	10	187	*Energy Environ. Sci.* **2013**, *6*, 2921.
Ni-doped Co_3O_4	1.0 M KOH	10	530	*Chem. commun.* **2013**, *49*, 7522.
NG-NiCo	1.0 M KOH	~	Onset overpotential 0.35 V	*Angew. Chem. Int. Ed.* **2013**, *52*, 13567.

Table S4 Comparison of selected non-noble metal based bifunctional electrocatalysts in alkaline media.

Catalysts	Electrolyte	j (mA cm^{-2})	η (V)	Reference
NiO@Ni/WS_2/CC	1 M KOH	10	1.42	This work
NiSe	1 M KOH	10	1.63	*Angew. Chem. Int. Ed.* **2015,** *54*, 9351.
Ni_5P_4	1 M KOH	10	1.70	*Angew. Chem. Int. Ed.* **2015,** *54*, 12361.
Ni_2P	1 M KOH	10	1.63	*Energy Environ. Sci.* **2015,** *8*, 2347.
CoMnO@CN	1 M KOH	10	~1.5	*J. Am. Chem. Soc.* **2015,** *13,* 14305.
CoO_x@CN hybrids	1 M KOH	20	1.55	*J. Am. Chem. Soc.* **2015**, *137,* 2688.
$CoNi(OH)_x$	1 M KOH	11	1.65	*Adv. Energy Mater*. **2016**, *6*, 1501661.
Co-P film	1 M KOH	100	1.744	*Angew. Chem. Int. Ed.* **2015**, *54,* 6251.
CoP_2/RGO	1 M KOH	10	1.56	*J. Mater. Chem. A.* **2016,** *4*, 4686.

Reference:

1. Gao, L.; Wang, X.; Xie, Z.; Song, W.; Wang, L.; Wu, X.; Qu, F.; Chen, D.; Shen, G. High-performance energy-storage devices based on WO_3 nanowire arrays/carbon cloth integrated electrodes. *J. Mater. Chem. A* **2013**, *1*, 7167–7173.